Synthesis, Spectral and Toxicological Studies of Complex Zn(II) with Sulfadiazine

[a]P. GURU*, [a]R. K. GAUTAM, and [b]M. P. GOUTAM

[a]*Department of Chemistry, Dr. H . S. Gour University, Sagar, Madhya Pradesh, India 470001*
e-mail: pranayguru@rediffmail.com

[b]*State Forensic Science Laboratory, Raipur, Chhatisgarh, India*

Received 9 June 2003
Accepted for publication 16 June 2004

The present paper deals with the spectral and toxicological studies of the complex Zn(II) with antibiotic drug sulfadiazine (2-(*p*-aminobenzenesulfonamido)pyrimidine), a general formula $Zn(C_{10}H_{10}N_4O_2S)\cdot MoO_4\cdot H_2O$ has been suggested for the complex under study. The geometries of the complexes have been proposed on the basis of magnetic moments, electronic and infrared spectral data. Thermogravimetric analyses have been carried out to determine the pattern of their decomposition. The crystal system, lattice parameters, unit cell volume, and number of molecules in it have been determined by X-ray diffraction data.

The toxicity of the synthesized complex was also studied on some internal organs of the albino rats like liver, kidney, adrenal gland, and testis.

In continuation of the work on the metal molybdate/tungstate/vanadate complex with organic ligand, the present paper describes coordination behaviour of zinc(II) with sulfadiazine ($C_{10}H_{10}N_4O_2S$)

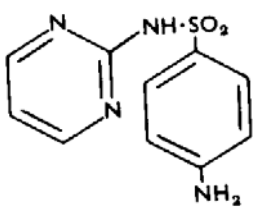

having molybdate as anion. The complex has been synthesized and characterized using analytical and spectral methods and its toxic behaviour was also studied on the internal organs of albino rats.

The data of analysis of the prepared complex are shown in Table 1. Synthesized complex is white in colour. Molecular formula of the complex has been worked out on the basis of the above data to be $Zn(C_{10}H_{10}N_4O_2S)MoO_4\cdot H_2O$. Zn complex is insoluble in water and soluble in common organic solvent, which indicates nonelectrolyte nature of this complex [1].

The Zn(II) complex under study shows a two-step decomposition pattern. The mass loss of data at the end of the first step corresponds to the removal of one water molecule in the Zn(II) complex in the temperature range 300—410 K. The second step corresponds to the loss of ligand molecule from this complex in the temperature range of 450—910 K. The magnetic moment of the Zn(II) complex is diamagnetic.

The IR spectra (Table 2) of all complexes under study show a broad band at $\tilde{\nu} = 3450$ cm^{-1} and another band between 1600—1650 cm^{-1} which may be assigned to asymmetric and symmetric O—H stretching and H—O—H bending modes, respectively, indicating the presence of water of crystallization in the complexes. In the spectra of the complexes of sulfadiazine the bands displayed by the ligand at 1670 cm^{-1}, 1472 cm^{-1}, and 1380 cm^{-1} assignable to ν(C═O), ν(C—CH_2) (asymmetric), and ν(CH_2) (symmetric) remained unchanged in the complex, ruling out the possibility of involvement of the carboxyl oxygen in the metal binding.

The IR spectra of sulfadiazine and its analogous compounds have been characterized [4, 5]. The NH_2 group gives two absorption bands in the region 3300—3500 cm^{-1}. The first of these bands is due to asymmetric stretching and is usually found near 3500 cm^{-1}. In the present case, two bands obtained at 3445 cm^{-1} and 3380 cm^{-1} for the drug can be assigned to these two vibrations. In the metal complexes, asymmetric and symmetric bands are shifted to lower frequencies by 10—20 cm^{-1} and 15—17 cm^{-1}, respectively,

**Present address*: Dr. Pranay Guru c/o Dr. A. K. Guru, Near P. T. C. Ground, Gopalganj, Sagar, Madhya Pradesh, India 470001.

Table 1. Analytical Data of the Complex

M_r	w_i(calc.)/% w_i(found)/%					
	Zn(II)	MoO_4	C	H	N	S
749.91	8.717	21.861	32.003	2.933	14.935	8.543
	8.687	22.123	32.892	3.213	15.218	8.531

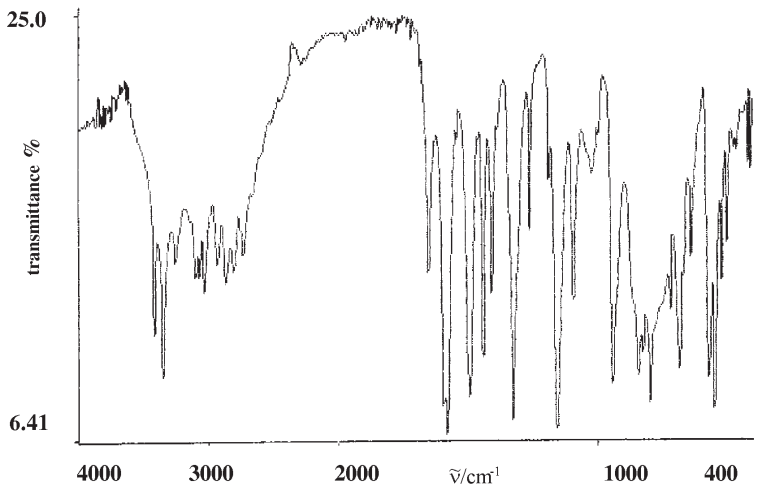

Fig. 1. Infrared spectrum of complex.

Table 2. Principle Wavenumbers ($\tilde{\nu}$/cm^{-1}) and their Assignment for Sulfadiazine and its Complex

Ligand	Complex	Assignment
3445 sh	3428 br	ν (NH_2)
3380 s	3357 br	
2950 s	2939 s	ν (C—H of CH_3)
2872 s	2872 s	
1670 m	1653 vs	C═O
1610 s	1599 w	Benzene ring
1472 w	1493 sp	C—CH_3 (asym)
1380s	1408 vs	C—CH_3 (sym)
1342 sh	1333 sp	C_6H_4—NH_2
1330 s	1326 w	SO_2N (asym)
1140 s	1157 vs	SO_2N (sym)
1080 s	1093 w	Substituted benzene ring
1030 s	1021 sh	
835 ms	843 sh	
	525 s	M—N
	499 w	M—O
	938 w	M—S

br = broad, m = medium, s = sharp, ms = medium sharp, w = weak, sh = shoulder, vs = very short.

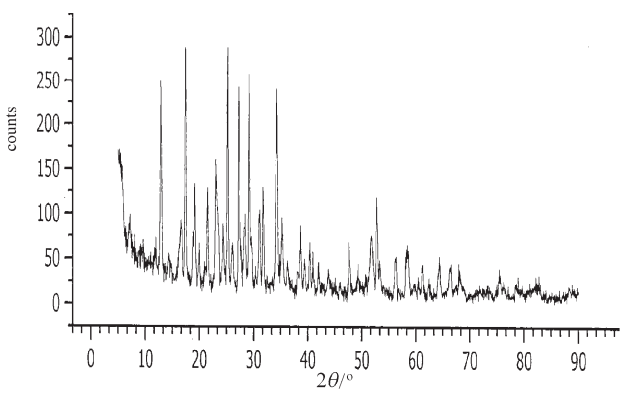

Fig. 2. X-Ray diffractogram of complex.

suggesting the involvement of the amino nitrogen in chelation. The involvement of NH_2 is confirmed by the IR data of NH_2 in sulfadiazine observed at 1622 cm^{-1}. These are shifted to lower frequencies in the metal complexes due to chelation. An overall range of 3050—3500 cm^{-1} has been assigned to the free NH vibration. In the far-infrared region combined frequencies of two metal nitrogen bands were observed around 480—510 cm^{-1} (Fig. 1).

The X-ray diffraction data of the complex in Tables 3, 4 and Fig. 2 show 43 peaks for Zn(II) complex clearly indicating the crystalline nature of complex. The X-ray pattern was changed by the trial-and-error method [6, 7] keeping in mind the characteristics of the various symmetry systems, until a good fit was obtained between the observed symmetry and the calculated sin θ values. The unit cell parameters were calculated from indexed data. It is also clear from the data that all prepared complexes possess tetragonal symmetry. The calculated and experimental value of

Table 3. Crystal Parameters and Density of the Complex

Crystal lattice edge			Cell volume	n	Density obs.	Density calc.	Crystal system
$a/Å$	$b/Å$	$c/Å$	$Å^3$		g cm^{-3}	g cm^{-3}	
23.8394	23.8394	15.2963	8693.2164	27	3.396	3.352	Tetragonal

Table 4. X-Ray Powder Diffraction Data of Complex

Peak No.	Spacing $d/Å$	Relative intensity $I/I_0 \times 100$	Observed Sin^2 θ	Calculated Sin^2 θ	(h k l)
1	15.30390	53.4	0.00253	0.00253	(1 0 0)
2	12.23475	34.1	0.00393	0.00393	(1 0 1)
3	6.84281	86.6	0.01262	0.01260	(0 0 3)
4	6.17561	19.3	0.01515	0.01514	(1 0 3)
5	5.33138	32.1	0.02075	0.02072	(2 2 0)
6	5.07544	99.7	0.02245	0.02241	(0 0 4)
7	4.70382	27.6	0.02495	0.02495	(1 0 4)
8	4.63079	46.2	0.02745	0.02748	(1 1 4)
9	4.44639	23.1	0.03095	0.03094	(3 1 2)
10	4.21710	14.1	0.03289	0.03288	(2 2 3)
11	4.11989	44.5	0.03505	0.03503	(0 0 5)
12	3.84617	55.5	0.03750	0.03756	(1 1 5)
13	3.78252	31.0	0.04140	0.04313	(2 2 4)
14	3.64929	30.7	0.04440	0.04447	(4 1 1)
15	3.52958	100.0	0.04867	0.04868	(4 1 2)
16	3.40939	23.4	0.05297	0.05297	(1 1 6)
17	3.26636	84.1	0.05567	0.05568	(4 1 3)
18	3.14489	34.5	0.06035	0.06038	(3 1 5)
19	3.05855	89.3	0.06311	0.06310	(2 1 6)
20	2.87784	41.3	0.07117	0.07118	(1 1 7)
21	2.81597	57.3	0.07578	0.07577	(3 1 6)
22	2.61582	99.5	0.08893	0.08892	(2 2 7)
23	2.54587	39.7	0.09123	0.09122	(6 0 0)
24	2.47461	19.8	0.09603	0.09604	(3 3 6)
25	2.33097	36.0	0.10355	0.10351	(4 4 4)
26	2.28335	20.7	0.11175	0.11174	(4 1 7)
27	2.23230	28.5	0.11632	0.11631	(5 1 6)
28	2.20014	24.0	0.12417	0.12416	(7 0 0)
29	2.15049	19.0	0.12811	0.12810	(5 1 0)
30	2.06472	16.1	0.13882	0.13882	(1 1 9)
31	1.90505	27.7	0.16174	0.16173	(5 5 5)
32	1.84701	18.6	0.17926	0.17936	(5 1 9)
33	1.76354	31.4	0.19466	0.19456	(4 4 9)
34	1.73378	49.2	0.20489	0.20487	(6 6 4)
35	1.63311	21.9	0.21626	0.21636	(5 5 8)
36	1.57966	27.3	0.24029	0.24019	(5 5 7)
37	1.51356	18.2	0.25209	0.25109	(6 6 7)
38	1.48606	12.0	0.26154	0.26144	(7 7 3)
39	1.44697	21.9	0.28356	0.28336	(7 7 5)
40	1.40678	17.4	0.29877	0.29876	(7 7 6)
41	1.37650	15.7	0.32994	0.32995	(8 8 2)
42	1.25840	16.5	0.37479	0.37478	(8 8 6)
43	1.21665	9.9	0.39298	0.39299	(8 8 7)

density of the complex is in good agreement within the limits of experimental error.

On the basis of the above studies in Fig. 3 is suggested the structure for the studied complexes.

Several pathological changes like the increase in the size of hepatocytes, clumping and margination of basophil granules, vacuolated cytoplasm of liver cells, *etc.* are known. In the present study, histopathological changes such as space were formed in between the hepatic cords, whereas hepatic cell showed pycnotic and degenerated nuclei and vacuolations. Blood haemorrhages were also observed. Kidney serves as one of the most important excretory organs in the mammals. Several pathological changes like necrosis, hy-

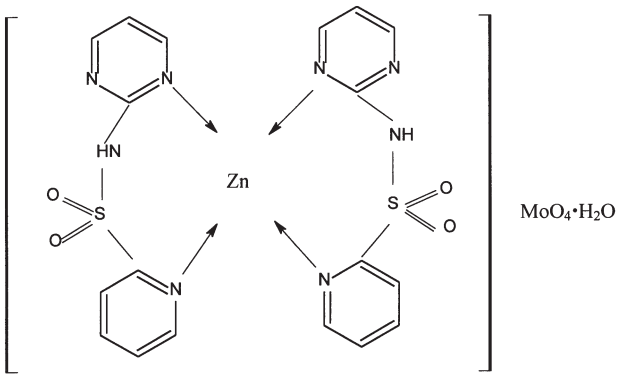

Fig. 3. Representative structure of the complexes.

pertrophy, space formation, and shrunken glomerules are reported due to toxic effect of metallic poisons. In the present study of testis, seminiferous tubules were hypertrophied. Germinal epithelial lining was damaged at some places and mature sperms were also necrotic. There was shrinkage of sertoli cells, spermatogonia, primary and secondary spermatocytes and spermatids due to which spaces were formed in the lobules.

Wong and *Klassen* [8] reported necrosis and atrophy in the testis of rat during cadmium toxicity. In the present study, similar changes were noticed with the complex under study. Seminiferous tubules were hypertrophied. Germinal epithelial lining was damaged at some places and mature sperms were also necrotic. There was shrinkage of sertoli cells, spermatogonia, primary and secondary spermatocytes and spermatids due to which spaces were formed in the lobules.

Adrenal medullary tumour in mice was reported by *Smith* and *Pilgrim* [9] after treatment with X-rays, stilbestrol or istradiol benzoate, progesterone, testosterone, and gonadotropic extracts. *Platt* and *Steward* [10] described that zona fasciculata of the adrenal cortex was usually less severely affected by protein caloric deficiency in pigs. Significant pathological changes in zona fasciculata of adrenal glands of rats after treatment by lead acetate were reported by *Roychowdhury et al.* [11]. In the present study, the zona fasciculata of cortex showed ruptured cells with pycnotic nuclei and vacuolation. Some of the cells became necrotic and spaces were also noticed in between the cord of cells. In medulla region, chromaffin cells were hypertrophied due to which spaces were formed and the cell became vacuolated at some places. All these changes showed that the complex if given for a longer period may show marked toxic symptoms due to the metallic ligands attached to it.

EXPERIMENTAL

The starting material $ZnMoO_4 \cdot H_2O$ was synthesized using the reported methods [12—14]. The complex was isolated by shaking $ZnMoO_4 \cdot H_2O$ (0.01 mol) with a required amount of $C_{10}H_{10}N_4O_2S$ (0.03 mol) in water ($\approx$ 100 cm^3). The products were filtrated, washed 3—4 times with ether and dried. The metal was estimated by various methods [15, 16].

Elemental analysis of the prepared complex was carried out in Lab-India and ASCHO laboratory, Mumbai, India. X-Ray diffraction (XRD) and thermogravimetric analysis (TGA) of the prepared complex was carried out at the Inter University Consortium, Indore, India. KBr pellets were used in FTIR spectral analysis.

At the determination of toxicity ten healthy albino rats were obtained from the veterinary college Mhow, India. They were kept in clean cages in the laboratory and fed on diet rich in carbohydrates and proteins such as rice, wheat, and grams. Albino rats weighing 150—200 g were selected for experimental work. Liver, kidney, adrenal gland, and testis of the albino rats were selected for the present study.

Two rats served as a control, and remaining five rats in each group were served to show the effect of the above stated complex for 8 weeks. The synthesized complex was given at the dose of 30 mg/kg body mass in corn oil orally. Simultaneously, controls were given corn oil alone. The above stated dose was given for 5 days/week for 8 weeks.

The animals were dissected 24 h after the last dose. Liver, kidney, adrenal gland, and testis were dissected out. After washing the organs in saline water, they were cut into pieces and kept in aqueous Bouin's fluid for 24 h. After 24 h, organs were taken out of Bouin's fluid and washed several times in tap water to remove the excess of picric acid. The small tissues were kept in different grades of alcohol, *viz.* 30 %, 50 %, 70 %, and 90 % absolute alcohol, for 15—20 min in each grade. Then, the tissues were transferred in 50 % xylene solution. After 15—20 min, the tissues were kept in 100 % xylene for 5—10 min and paraffin blocks were prepared.

Sections were cut at 6 μm. Sections were spread over the slide containing Mayer's albumin layer. After dehydration and staining the slide with hematoxylin and eosin stain, sections were observed under microscope and finally photomicrographs were taken.

Observations

During the experimental period, the control rats were found completely normal, having no fear and no body mass loss was observed. Abnormal behaviour was seen throughout the experimental work with the rats, some sluggishness, lethargic movements were observed in a few experimental animals besides a little mass loss.

The hepatic cells in comparison with the control liver (Fig. 4) were found to be ruptured with vacuolations. Pycnotic and degenerated nuclei were seen. At

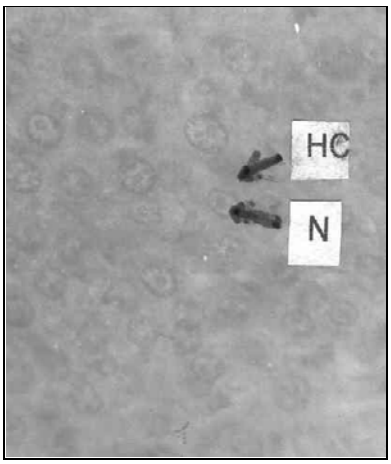

Fig. 4. Control liver. HC = hepatic cell, N = nucleus.

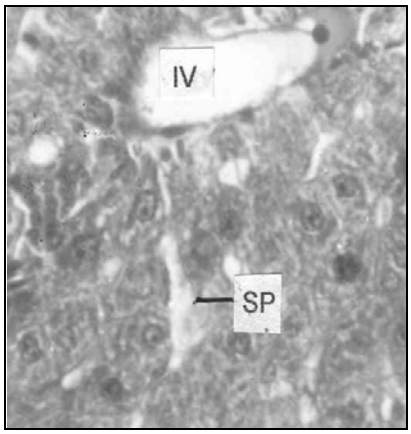

Fig. 5. Effect of complex in the liver of albino rat. IV = interlobular vein, SP = space.

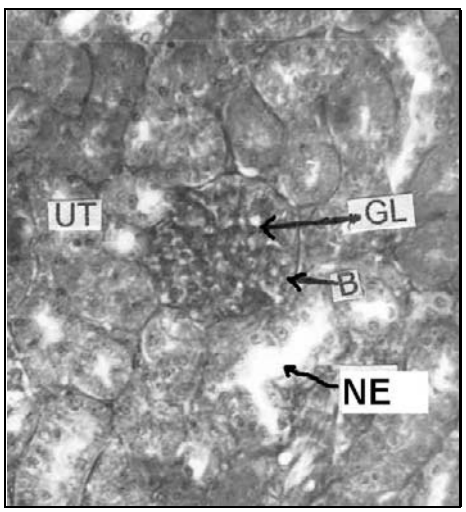

Fig. 6. Control kidney. B = Bowman's capsule, UT = uriniferous tubules, GL = glomerulus, NE = necrotic.

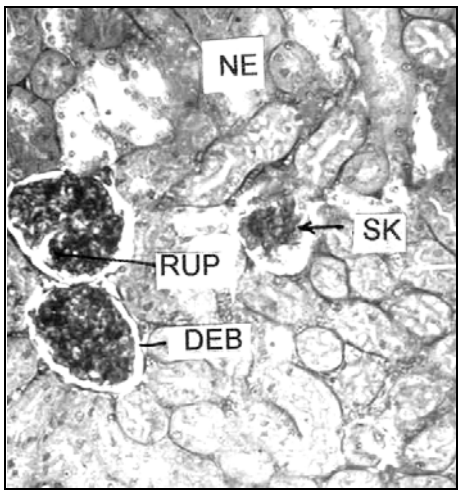

Fig. 7. Effect of complex in the kidney of albino rat. DEB = damage of epithelial lining of Bowman's capsule, RUP = ruptured, SK = shrinkage, NE = necrotic.

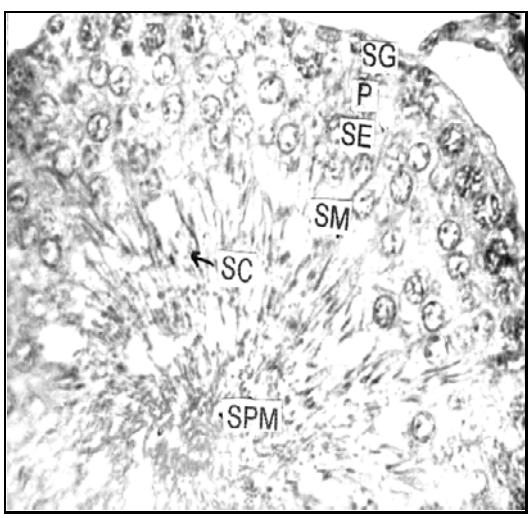

Fig. 8. Control testis. P = primary spermatocytes, SC = secondary spermatocyte, SG = spermatogonia, SM = spermatid, SPM = sperm.

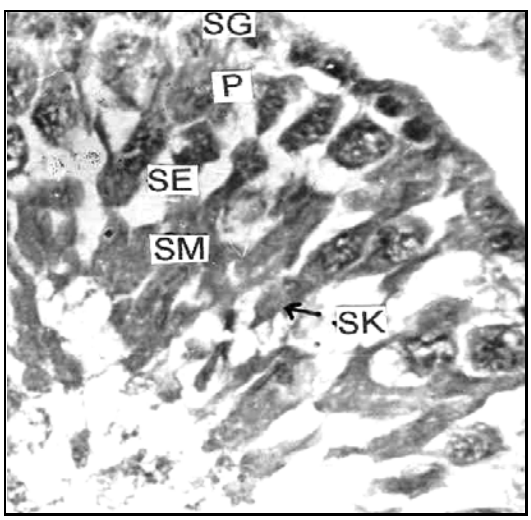

Fig. 9. Effect of complex in the testis of albino rat. Denotations as in the previous figures.

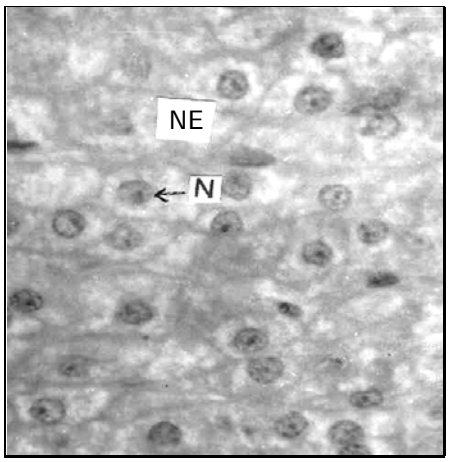

Fig. 10. Control. N = nucleus, NE = necrotic.

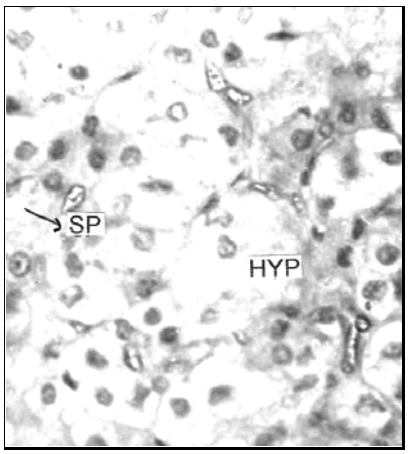

Fig. 11. Control. HYP = hypertrophy, SP = space.

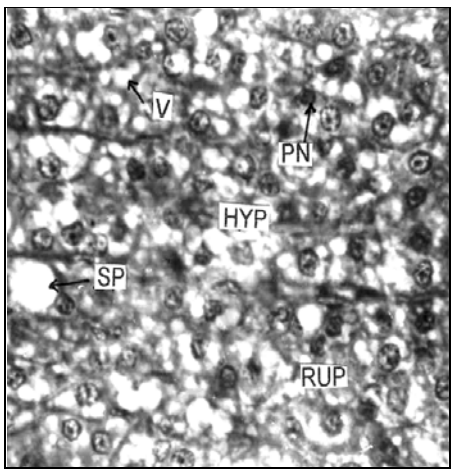

Fig. 12. Effect of complex in the adrenal gland of albino rat. PN = pycnotic nuclei, RUP = ruptured, V = vacuolation.

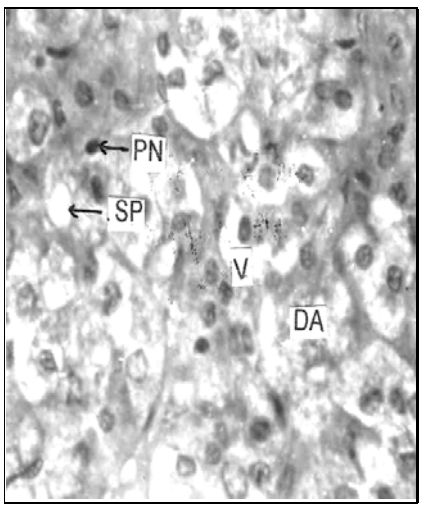

Fig. 13. Effect of complex in the adrenal gland of albino rat. DA = damage.

places binucleated cells were also seen. Spaces between the hepatic cords were noticed. Necrosis in hepatic cell and hypertrophied intralobular vein was observed (Fig. 5).

In comparison with the histological structure of simultaneous controls kidney (Fig. 6) Bowman's capsule was ruptured whereas its epithelial lining was disintegrated. Collecting tubules and the renal tubules showed dilation and vacuolation, respectively (Fig. 7).

In comparison with control (Fig. 8), there was shrinkage of sertoli cells, spermatogonia, primary and secondary spermatocytes and spermatids due to which spaces were formed in the lobules. Spermatids and sperms were displaced and degenerated showing vacuolation (Fig. 9).

In comparison with control (Figs. 10 and 11), the zona fasciculata of cortex resulted in ruptured cells with pycnotic nuclei and vacuolation. Space formation was also noticed. In medulla region, the chromaffin cells became hypertrophied and shrunken resulting in space formation. The chromaffin cells with pycnotic nuclei and vacuolation were observed (Figs. 12 and 13).

Acknowledgements. The authors are thankful to Dr. A. K. Guru, Director, State Forensic Science Laboratory, Sagar (M.P.), India and Dr. V. K. Saxena, Professor and Head, Department of Chemistry, Dr. H. S. Gour University, Sagar (M.P.) for providing necessary laboratory facilities and valuable suggestions. The authors are also thankful to Dr. Bhawalkar, Director, and Dr. V. K. Wadhawan, Head, Laser and Material Division, Centre for Advanced Technology, Indore, and Dr. Ajay Gupta, Centre Director, Inter University Consortium, Indore (M.P.) for permission to use the instrumental facilities at their laboratories.

REFERENCES

1. Glasstone, S., *An Introduction of Electrochemistry*, 2nd Edition, p. 70. McMillan, New Delhi, 1956.
2. Lever, A. B. P., *Inorganic Electronic Spectroscopy*, 2nd Edition, p. 112. Elsevier, New York, 1968.
3. Dutta, R. L. and Syamal, A., *Elements of Magneto-*

chemistry, 2nd Edition, pp. 100—102. S. Chand and Co., New Delhi, 1993.
4. Mills, T., Roberson, J. C., McCurdy, H. H., and Wall, W. H., *Instrumental Data for Drug Analysis*, 2nd Edition, pp. 2116—2117. CRC Press, Boca Raton, New York, 1993.
5. Moffat, A. C., Jackson, J. V., Moss, M. S., and Widdop, B., *Clarke's Isolation and Identification of Drugs,* p. 983. The Pharmaceutical Press, London, 1986.
6. Henary, N. F. M., Lipson, H., and Wooster, W. A., *X-Ray Diffraction Photographs*, p. 179. McMillan, London, 1959.
7. Peiser, H. S., Rooksky, H. P., and Wilson, A. J. C., *X-Ray Diffraction by Polycrystalline Materials,* p. 344. Institute of Physics, London, 1955.
8. Wong, K. L. and Klassen, C. D., *Toxicol. Appl. Pharmacol. 55*, 456 (1980).
9. Smith, C. S. and Pilgrim, H. I., *Cancer Res. 9*, 193 (1949).
10. Platt, B. S. and Steward, R. J. C., *J. Endocrinol. 38*, 121 (1967).
11. Roychowdhury, A., Bhatt, H. V., and Gautam, A. K., *J. Environ. Biol. 5*, 61 (1984).
12. Gupta, C. and Gautam, R. K., *Rev. Inorg. Chem. 20*, 241 (2000) and Guru, P., Goutam, M. P., and Gautam, R. K., *Main Group Met. Chem. 26*, 141 (2003).
13. Mellor, J. W., *A Comprehensive Treatise of Inorganic and Theoretical Chemistry*, 11th Edition, p. 802. Longman, London, 1947.
14. Gupta, C. and Gautam, R. K., *Indian J. Chem. 41(A)*, 763 (2002).
15. Vallance, R. H., Twiss, D. F., and Russell, A. R. A., *Textbook of Inorganic Chemistry*, p. 383. Charles Griffin, London, 1931.
16. Vogel, A. I., *A Textbook of Quantitative Inorganic Analysis*, 4th Edition, pp. 531, 527, 497, 302, 324. Longman, London, 1961.